Published in final edited form as:
Arch Biochem Biophys. 2008 September 15; 477(2): 285–290. doi:10.1016/j.abb.2008.07.011.

Role of the conserved distal heme asparagine of coral allene oxide synthase (Asn137) and human catalase (Asn148): mutations affect the rate but not the essential chemistry of the enzymatic transformations

Benlian Gao, **William E. Boeglin**, and **Alan R. Brash**
Department of Pharmacology and the Vanderbilt Institute of Chemical Biology, Vanderbilt University, Nashville, TN 37232, U.S.A.

Abstract

A catalase-related allene oxide synthase (cAOS) and true catalases that metabolize hydrogen peroxide have similar structure around the heme. One of the distal heme residues considered to help control catalysis is a highly conserved asparagine. Here we addressed the role of this residue in metabolism of the natural substrate 8R-hydroperoxyeicosatetraenoic acid by cAOS and in H_2O_2 breakdown by catalase. In cAOS, the mutations N137A, N137Q, N137S, N137D, and N137H drastically reduced the rate of reaction (to 0.8–4% of wild-type), yet the mutants all formed the allene oxide as product. This is remarkable because there are many potential heme-catalyzed transformations of fatty acid hydroperoxides and special enzymatic control must be required. In human catalase, the N148A, N148S, or N148D mutations only reduced rates to ~20% of wild-type. The distal heme Asn is not essential in either catalase or cAOS. Its conservation throughout evolution may relate to a role in optimizing catalysis.

Keywords

Peroxidase; Distal heme; Enzyme kinetics; HPETE; Hydroperoxyeicosatetraenoic acid; Hydrogen peroxide; Allene oxide; Allene oxide synthase; Catalase

Catalases eliminate hydrogen peroxide by utilizing one H_2O_2 molecule for heme activation to Compound I and a second H_2O_2 molecule for heme reduction back to the resting state, in the process converting $2H_2O_2$ to $2H_2O$ plus O_2. Currently there are hundreds of catalase sequences in the databases, identified through their sequence similarities [1–4]. Their common structural features comprising the catalase fold include the conserved sequence context of three significant amino acids around the catalytic heme in the active site. In order of appearance in the protein sequence, the first is a conserved histidine (His75 using the numbering for human catalase) that resides over the distal side of the heme and that is viewed as essential to catalysis [5,6] (Figure 1, left hand side). The distal side of the heme also includes a conserved asparagine (Asn148) positioned over the heme near to His75 [6]. This residue is often implicated along

Corresponding author: Alan R. Brash, Dept. of Pharmacology, Vanderbilt University School of Medicine, 23rd Ave. S. at Pierce, Nashville, TN 37232-6602. Tel.: 615-343-4495; Fax: 615-322-4707; E-mail: alan.brash@vanderbilt.edu.

with the distal His in modulating or tuning catalysis, and its role is the focus of this study. In bacterial large (75–84 kDa) subunit monofunctional catalase HPII, mutation of the equivalent distal heme Asn is associated with reduced catalatic activity [7]. The third conserved amino acid in order of appearance in the sequence is the proximal heme ligand, a tyrosine (Tyr388) in the sequence context of Arg-(three hydrophobic residues)-Tyr-(six residues)-Arg. The Arg residues help brace the Tyr on the underside of the heme. Taken together, in the correct sequence context, these three amino acids are conserved as part of the signature sequence of catalases.

In addition to the ubiquitous true catalases, there are a few organisms that express an additional catalase-related protein that utilizes a substrate other than hydrogen peroxide. We characterized the first of these a decade ago when we identified the heme domain of a natural fusion protein as a catalase-related allene oxide synthase (cAOS) [8]. cAOS transforms the lipoxygenase product 8*R*-HPETE (8*R*-hydroperoxyeicosatetraenoic acid) to the allene epoxide, 8,9-epoxyeicosa-5Z,9,11Z,14Z-tetraenoic acid (Scheme) [8,9]. Allene oxides are unstable epoxides that are intermediates in the biosynthetic pathways of corals and plants [10]. The fatty acid hydroperoxide 8*R*-HPETE is synthesized from arachidonic acid by the lipoxygenase that is encoded as the C-terminal domain of the fusion protein with the catalase-related AOS at the N-terminus. The recent characterization of the X-ray crystal structure of this heme domain revealed a remarkable similarity to the central core structure of catalase (Figure 1, right side) [11]. However, quite remarkably the coral catalase-related domain exhibits no reaction with H_2O_2 [9,12]. From recent studies we know that this coral catalase-related/LOX fusion protein is not unique. For example, our group and others reported on a cyanobacterial catalase-related/LOX fusion protein that forms allylic epoxides from C18 fatty acid substrates [13–15].

The chemistry of allene oxide synthesis catalyzed by the coral AOS (cAOS) is analogous to the reaction of the plant AOS that convert C18 fatty acid hydroperoxides to allene oxides. The plant AOS are members of the CYP74 family of cytochromes P450 [16,17]. The CYP74 family includes enzymes that metabolize the same C18 fatty acid hydroperoxide substrates to a number of different products [18]. Thus CYP74A encodes AOS enzymes [17,19–22], CYP74B are hydroperoxide lyases [23], CYP74C includes both AOS and lyases [24], and CYP74D comprises divinyl ether synthases [25]. All of these CYP74 enzymes share at least 35% amino acid sequence identity. With this knowledge in mind, we questioned whether the coral AOS has the potential to be converted into a hydroperoxide-metabolizing enzyme with a different catalytic specificity. With the understanding that reaction is catalyzed on the distal side of the heme, we hypothesized that changes in the distal heme environment might affect the chemistry of fatty acid hydroperoxide transformation. Accordingly we have explored the influence of the distal heme Asn in cAOS and for comparison with a true catalase, in the distant relative human catalase.

Materials and methods

Materials

Arachidonic acid (AA) was purchased from NuChek Prep Inc (Elysian, MN), and 8*R*-HPETE was synthesized using 8*R*-LOX [9]. H_2O_2 was from Fisher Scientific.

Construction of expression vectors

The construction of allene oxide synthase was described in the previous studies [9]. Human catalase was cloned from tonsil tissue. Firstly, human catalase cDNA was PCR-amplified using the primers 5'*CAT* **ATG** GCT GAC AGC CGG GAT CCC GCC 3' and 5' *GAT ATC* **TCA** GTG ATG GTG ATG GTG ATG CAG ATT TGC CTT CTC CCT TGC CGC 3', thereby adding a C-terminal His tag before the stop codon and including *Nde* I and *Eco*R V restriction sites at

N-terminal and C-terminal ends respectively. The DNA sequencing confirmed the correct cloning of human catalase. Then the human catalase gene was sub-cloned into pET17b expression vector (Invitrogen). Plasmids containing the correct insert were transformed into *E. coli* BL21(DE3) cells for the expression of human catalase.

Site-directed mutagenesis for cAOS and Human catalase

Site-directed mutagenesis for cAOS and human catalase were generated utilizing the QuikChange Site-Directed Mutagenesis Kit (Stratagene, Cedar Creek, TX, USA) following the manufacturer's instructions. Wild type plasmids were used as templates, and point mutation primers designed as in Table 1 were added to the PCR reaction. After the PCR reaction, the amplified products were digested with *Dpn* I restriction enzyme to remove parental DNA, the mutant constructs were transformed into DH5α cells for the amplification of plasmid DNA. Consequently, plasmids were extracted by Wizard® *Plus* SV Miniprep DNA purification system (Madison, WI, USA) from a 2 mL overnight growth culture and submitted for sequencing. All point mutations were verified by DNA sequencing (Vanderbilt University). Plasmids containing the correct insert were transformed into BL21(DE3) expression cells for expression of the mutant proteins.

Bacterial Expression of cAOS, catalase and their mutants

Protein expression were carried out in BL21(DE3) cells using a modified method described by Hoffman *et al* [26] and Boutaud *et al.*[9]. The cells were harvested at 5,000 × g for 15 min in a Sorvall RC-3 centrifuge, washed with 25 ml of 50 mM Tris, pH 7.9, pelleted again at 5,000 × g for 20 min, and resuspended in 10 ml of TSE buffer (100 mM Tris acetate, pH 7.6, 500 mM sucrose, 0.5 mM EDTA) containing 1 mg/ml lysozyme and kept on ice for 30 min. and spun down at 5,000 × g for 20 min. The pellets were frozen at −80 °C for later use.

Purification of His-tagged Proteins

The histidine-tagged cAOS or catalase or their mutants were purified following the protocol of Imai *et al.* [27] and Boutaud *et al.* [9] with some modifications. The pellet was resuspended in BugBuster® Protein Extraction Reagent (Novagen) by sonication, and homogenized with glass homogenizer. The 16,000 × g supernatant was loaded on a nickel-NTA column (0.5 ml bed volume, Qiagen) equilibrated with 50 mM potassium phosphate buffer, pH 7.2, 500 mM NaCl at 0.5 ml/min. The column was then washed with the equilibration buffer and the nonspecific bound proteins were eluted with 50 mM potassium phosphate buffer, pH 7.2, 500 mM NaCl, 70 mM glycine. A final wash was performed by 50 mM potassium phosphate buffer, pH 7.2, 500 mM NaCl, 20 mM imidazole. The His-protein was then eluted with 50 mM potassium phosphate buffer, pH 7.2, 500 mM NaCl, 250 mM imidazole. Fractions of 0.5 ml were collected and assayed for the AOS or catalase activity. Up to this point all procedures were the same for cAOS and catalase. The cAOS positive fractions were pooled and dialyzed overnight against 50 mM Tris buffer, pH 7.9, 500 mM NaCl, 20% glycerol and aliquoted and frozen in −80 °C for later use. Catalase fractions were pooled and dialyzed twice against 2 L buffer (20 mM Tris, pH 7.5) to get rid of salt for Mono Q column purification by FPLC. The Mono Q column was pre-equilibrated with 20 mM Tris buffer pH 7.5, and loaded with catalase fractions. The gradient was set 0–250 mM NaCl with flow rate of 1 ml/min. The fractions were monitored by UV detector and confirmed pure by SDS-PAGE.

Incubation and extraction conditions

30 μg 8*R*-HPETE was incubated with an appropriate amount of cAOS enzyme or its mutants in 3 ml of 50 mM Tris buffer, pH 7.5, 150 mM NaCl for 3 min, then acidified with 0.6 ml of 1M KH_2PO_4 solution, 30 μl of 1N HCl to reach a pH of 4–5. Products were extracted by 1ml C18 HLB Cartridge (Waters OASIS®). The column was prepared by running methanol first

and then with water. Products were loaded onto the column, washed with water and eluted with methanol.

HPLC analysis of cAOS products

Extracts were dried under a stream of nitrogen and redissolved in HPLC solvent. Analyses were carried out by RP-HPLC using a Waters Symmetry C18 column (25 × 0.46 cm), a solvent system of methanol/water/acetic acid in the proportions 80/20/0.01 (v/v/v), a flow rate of 1 ml/min, with UV detection at 205 nm, 220 nm, 235 nm and 270 nm using an Agilent 1100 series diode array detector.

Activity assays

The AOS and its mutants were assayed by following the decrease in absorbance at 235 nm due to the breakage of hydroperoxides in 50 mM Tris buffer, pH 7.5, 150 mM NaCl using a Lambda 35 UV/VIS spectrophotometer (PerkinElmer). The initial rate was expressed as nanomoles of hydroperoxides decomposed per nanomole of heme per second. Catalase and its mutants were assayed by measuring the decrease at 240 nm due to the consumption of H_2O_2 in 50 mM potassium phosphate buffer, pH 7.0, using a Lambda 35 UV/VIS spectrophotometer (PerkinElmer). Similarly, the initial rate was expressed as nanomoles of H_2O_2 decomposed per nanomole of heme per second.

Results

Expression and purification of human catalase and cAOS

Human catalase cDNA including a C-terminal His-tag was cloned into the expression vector pET17b and the protein was expressed in *E. coli* BL21(DE3) with a 36 mg yield of active protein per liter growth under the conditions described in Materials and Methods. cAOS expression yielded 110 mg protein per liter growth using the method described by Boutaud *et al* [9]. Mutants made by site-directed mutagenesis of the distal heme Asn in human catalase (Asn148) and cAOS (Asn137) were also expressed in *E. coli* BL21(DE3). In most cases proteins expressed well (20–100 mg/liter). The cAOS was purified using a Ni-NTA affinity column to greater than 90% homogeneity, except for the Asp and Leu mutants which had low levels of expression and gave impure preparations of enzyme (Figure 2). The N137L and the N137V mutants expressed with a low content of heme (<5%). Human catalase and its mutants were isolated using Ni-NTA affinity and further purified using Fast Protein Liquid Chromatography on a Mono-Q column; the proteins recovered from the Mono-Q column showed a single band on SDS-PAGE (Figure 3). UV/VIS spectroscopy indicated a high heme content as evidenced by an absorption ratio for $A_{406/280}$ of 1.2, better than the value of 1.04 reported for the human catalase used in X-ray crystallography [28]

Steady-state kinetic analyses of human catalase and its mutants

To identify the role of the distal Asn148, mutations were designed to change or eliminate the hydrogen bonding side chain in the active site. Replacement of Asn148 with Ala, Gln, Asp, and Ser each gave a protein with similar heme content to wild-type. The catalatic activities of wild type human catalase and the mutants were determined by spectrophotometric measurement of H_2O_2 consumption using the absorbance decrease at 240 nm [29]. The results in Figure 4 illustrate the initial rates measured up to a H_2O_2 concentration of 50 mM, the highest concentration compatible with this spectroscopic assay. Human catalase, like other true catalases, does not attain V_{max} at H_2O_2 concentrations up to 1–2 M [4]. That V_{max} is not attained is evident in the wild-type kinetics (Figure 4), whereas several of the mutants, in addition to exhibiting overall lower activity, also appear to reach close to maximal rates of reaction.

Table 2 summarizes the kinetic parameters obtained from the steady-state kinetic assay. The wild-type enzyme achieved a k_{cat} of ~4×10^5 per sec per heme moiety, in accord with published values [4]. The N148A, N148S and N148D mutants each gave ~5-fold lower values for k_{cat}, while the N148Q mutant displayed feeble catalytic activity, about 400-fold lower than wild-type. The estimated K_M of 72 mM for the wild type catalase is in good agreement with a previous report from human erythrocyte catalase (81 mM) [4]. There is a considerable decrease in K_M for the N148A, N148S and N148D mutants compared to wild type catalase (Table 2). This likely reflects the fact that the mutants reach near a maximal rate at 50 mM H_2O_2 concentration whereas the wild type has not even reached its estimated K_M at that point. As a consequence of the lower K_M, the catalytic efficiencies (k_{cat}/K_M) of the mutants compute to values similar to wild-type catalase.

Product analyses of cAOS and its mutants

To investigate the role of the distal heme residues in cAOS, we first checked the involvement of the distal His67 by its mutagenesis to Val or Asn. Both mutations resulted in protein with a low heme content and with zero cAOS activity (data not shown). To investigate the role of the distal Asn137, we prepared an extensive series of mutants to test the importance of hydrogen bonding, positive or negative charge, and space-filling/hydrophobicity; Asn137 was replaced with Ser, Gln, Asp, His, Lys, Ala, Val, or Leu. These proteins expressed well, with the exception of the N137V and N137L mutants, which exhibited a low content of heme.

Wild-type cAOS converts 8*R*-HPETE to the unstable 8,9-epoxy allene oxide, which is subject to almost instant non-enzymatic hydrolysis to the α-ketol 8-hydroxy-9-ketoeicosa-5,11,14-trienoic acid and lesser amounts of the γ-ketol 12-hydroxy-9-ketoeicosa-5,10,14-trienoic acid; non-enzymatic cyclization of the allene oxide also occurs and accounts for about 15–20% of the end products as a prostaglandin-like cyclopentenone (Scheme) [30]. These three degradation products of the allene oxide give a distinctive pattern on HPLC analysis with diode array detection (Figure 5A). Also, the transformation of 8*R*-HPETE is associated with loss of its conjugated diene chromophore, allowing assay of cAOS reaction rates by following the decrease in absorbance at 235 nm. As shown in Table 3, all the Asn137 mutant proteins displayed a severe loss in activity compared to wild-type. The N137A and N137Q retained the most activity (only ~4%), while the N137K (0.2%) and N137L (0.03%) showed the least.

Despite this major impact on activity, the Ser, Gln, Asp, and Ala mutants all showed an identical characteristic pattern of allene oxide-derived products on HPLC analysis, illustrated in Figure 5B for the N137A enzyme. The nature of the products was confirmed both by their distinctive HPLC-UV profiles at specific wavelengths and by their diagnostic UV spectra (Figure 5A, inset). The His mutant formed prominent allene oxide-derived products along with some non-specific reaction products such as 8,15-di(hydro)peroxides with conjugated triene chromophores (cf. ref. [31]) and a trace of a C13 aldehyde cleavage product of 8*R*-HPETE (cf. ref. [32]). The Val and Leu mutants formed barely detectable levels of allene oxide-derived products along with non-specific by-products similar in type to the His mutant. Only the N137K mutant formed no discernible allene oxide; instead, the HPLC chromatogram showed multiple products (more than 20), many with 205 nm absorbance, likely reflecting the non-specific transformation to mixtures of epoxyalcohol isomers and other rearrangements, a characteristic of non-specific heme-catalyzed breakdown of fatty acid hydroperoxides (data not shown) [33–35]. The important point, to re-state it, is that Asn mutations to Ser, Gln, Asp, Ala, His, Val, and Leu all resulted in enzymes capable of specific allene oxide synthesis from 8*R*-HPETE, albeit at a greatly reduced rate.

Discussion

The X-ray crystal structure of several catalases was determined in the 1980's, giving a good picture of the active site environment and the potential amino acid residues participating directly in catalysis [5,36–38]. The distal heme histidine, a residue conserved in monofunctional catalases, was deduced to be of vital importance and this was confirmed by mutagenesis in the 1990's [7]. From the time of the first crystal structures the distal heme Asn (N148 in human catalase) was also implicated in catalysis, and even relatively recently the Asn148 was featured prominently in the catalatic cycle [6]. For example, one proposed role for Asn148 was to cooperate with His75 in hydrogen bonding to one oxygen of H_2O_2 and thus increase affinity for the substrate [6]. Our results tend to show that, in the Asn148 mutants, high concentrations of H_2O_2 show very markedly reduced reaction rates whereas low concentrations are handled almost as well as in wild-type; the Asn148Ala mutant, for example, shows 70–80% of the reaction rate as wild type at H_2O_2 concentrations up to 10 mM. Kinetically these effects appear as a much lower V_{max} in the mutants, a lower K_M, and similar values for k_{cat}/K_M, reflecting the near-normal reaction rates with modest concentrations of H_2O_2. A potential explanation for these atypical kinetics is that the distal Asn helps promote reaction at the higher concentrations of H_2O_2, perhaps by binding substrate, and substitution of the Asn thus lowers V_{max}, as a consequence leading to a computed lower value for K_M. As noted in the Introduction, the equivalent Asn in a large subunit bacterial catalase (*E. coli* HPII) was mutated and shown to diminish but not abolish catalatic activity. We obtained a similar result here using human catalase, which is classified as a typical clade III small subunit catalase by the convention of Klotz and Loewen [2]. In both cases the Asn-to-Ala mutant retained appreciable activity, although distinctly lower than wild-type. With the different mutants, generally if heme was retained in the protein, so was catalytic activity. The idea that this fairly well-conserved residue is not essential to catalysis has emerged recently for a hemoprotein peroxidase. Thus, the peroxidase activity of ovine prostaglandin H synthase-1 was found to be retained in the Gln-to-Val mutant, indicating that the hydrogen bonding capability of distal heme Gln is not required [39].

While it is all but self-evident that allene oxide synthesis occurs in the heme active site of cAOS, direct proof of the reaction pathway is only partly demonstrated. Certainly, the X-ray structure of cAOS shows that the distal side of the heme is comparatively open and accessible compared to catalase [11], although so far there is no structure with a bound substrate analogue. Compound I, a key intermediate in catalysis, is observed in cAOS treated with peracetic acid [12]. Raman spectral data indicate that catalase adopts a 5-coordinate/high spin structure, whereas cAOS has purely a 6-coordinate/high spin heme. Significantly, an active site mutation on the residue adjacent to the distal heme His67 (Thr66Val) confers H_2O_2-metabolizing capacity on cAOS; this T66V mutant has a 5-coordinate/high spin heme as a minor species, and probably because of this it exhibits some catalatic activity [12]. The transformation of 8*R*-HPETE to allene oxide is understood in chemical terms (e.g. ref. [40]), but the step-by-step dissection of the reaction in cAOS has yet to be resolved.

In contrast to the breakdown of hydrogen peroxide, the chemical breakdown or rearrangement of fatty acid hydroperoxides has many potential outcomes, so there is a need for strict enzymatic control in the transformation to an allene epoxide. Indeed, in a half century of studies on the degradation of fatty acid hydroperoxides, in the course of which the degradation to multiple epoxides, aldehydes, ethers and alcohols has been documented [35,41,42], no evidence of *non-enzymatic* formation of allene oxides has ever been produced. The only known examples of allene oxide synthesis in biology are the enzymatic transformations catalyzed by the CYP74 cytochrome P450s and the equivalent reactions of the catalase-related AOS [10]. We also know that different members of the CYP74 family of enzymes display distinct catalytic activities, giving different products from the same fatty acid hydroperoxide substrate [18]. For all these

reasons we suspected that a marked alteration in the cAOS active site might disrupt the process of allene oxide synthesis and lead to another outcome. Surprisingly, however, the cAOS mutants with substitutions in the distal heme Asn did not form new products. Although their catalytic efficiencies were seriously impaired, retaining no more than 4% of wild type activity, most of mutants were able to catalyze the formation of allene oxide. Even the Asn137Ala mutant produced the allene oxide. Our previous assumption on the catalytic mechanism of allene oxide formation invoked a role for hydrogen bonding from the distal heme Asn137 [11], but our results shown here indicate that this can play no role in the specific transformation to the allene oxide product.

We conclude that the importance of the conserved distal heme Asn in catalase and catalase-related enzymes may have been overestimated, or at least misrepresented. The conserved Asn occupies a conspicuous position, and as the nearest hydrogen-bonding residue to the center of catalytic activity it seems obvious that it should play a crucial role in catalysis. It does function catalytically in speeding up the reaction rate ~5-fold in catalases and ~20 – 100-fold in AOS, although it is not essential in either enzyme. While crucial to an efficient reaction rate in cAOS, it plays no role in directing fatty acid hydroperoxide transformation to the allene oxide. It is clear from our results that the distal Asn optimizes reaction rate. Its conservation throughout evolution may relate to this role in optimization of the inherent catalytic activity.

Abbreviations footnote

AOS, allene oxide synthase; cAOS, catalase-related allene oxide synthase; LOX, lipoxygenase; H(P)ETE, hydro(pero)xyeicosatetraenoic acid; RP-HPLC, reversed-phase high pressure liquid chromatography; SP-HPLC, straight-phase high pressure liquid chromatography; Ni-NTA, nickel nitrilotriacetic acid.

Acknowledgements

This work was supported by NIH grant GM-74888 to A.R.B..

References

1. Chelikani P, Fita I, Loewen PC. Cell Mol Life Sci 2004;61:192–208. [PubMed: 14745498]
2. Klotz MG, Loewen PC. Mol Biol Evol 2003;20:1098–1112. [PubMed: 12777528]
3. Nicholls P, Fita I, Loewen PC. Adv. Inorg. Chem 2001;51:51–106.
4. Switala J, Loewen PC. Arch Biochem Biophys 2002;401:145–154. [PubMed: 12054464]
5. Murthy MR, Reid TJ 3rd, Sicignano A, Tanaka N, Rossmann MG. J Mol Biol 1981;152:465–499. [PubMed: 7328661]
6. Putnam CD, Arvai AS, Bourne Y, Tainer JA. J Mol Biol 2000;296:295–309. [PubMed: 10656833]
7. Loewen PC, Switala J, von Ossowski I, Hillar A, Christie A, Tattrie B, Nicholls P. Biochemistry 1993;32:10159–10164. [PubMed: 8399141]
8. Koljak R, Boutaud O, Shieh BH, Samel N, Brash AR. Science 1997;277:1994–1996. [PubMed: 9302294]
9. Boutaud O, Brash AR. J Biol Chem 1999;274:33764–33770. [PubMed: 10559269]
10. Tijet N, Brash AR. Prostaglandins Other Lipid Mediat 2002;68–69:423–431.
11. Oldham ML, Brash AR, Newcomer ME. Proc. Natl. Acad. Sci. U S A 2005;102:297–302. [PubMed: 15625113]
12. Tosha T, Uchida T, Brash AR, Kitagawa T. J Biol Chem 2006;281:12610–12617. [PubMed: 16513636]
13. Lang I, Gobel C, Porzel A, Heilmann I, Feussner I. Biochem J 2008;410:347–357. [PubMed: 18031288]

14. Schneider C, Niisuke K, Boeglin WE, Voehler M, Stec DF, Porter NA, Brash AR. Proc Natl Acad Sci U S A 2007;104:18941–18945. [PubMed: 18025466]
15. Zheng Y, Boeglin WE, Schneider C, Brash AR. J Biol Chem. 2007
16. Feussner I, Wasternack C. Annu Rev Plant Biol 2002;53:275–297. [PubMed: 12221977]
17. Song WC, Funk CD, Brash AR. Proc Natl Acad Sci U S A 1993;90:8519–8523. [PubMed: 8378325]
18. Grechkin AN. Prostaglandins Other Lipid Mediat 2002;68–69:457–470.
19. Laudert D, Pfannschmidt U, Lottspeich F, Hollander-Czytko H, Weiler EW. Plant Mol Biol 1996;31:323–335. [PubMed: 8756596]
20. Maucher H, Hause B, Feussner I, Ziegler J, Wasternack C. Plant J 2000;21:199–213. [PubMed: 10743660]
21. Pan Z, Durst F, Werck-Reichhart D, Gardner HW, Camara B, Cornish K, Backhaus RA. J Biol Chem 1995;270:8487–8494. [PubMed: 7721745]
22. Song WC, Brash AR. Science 1991;253:781–784. [PubMed: 1876834]
23. Matsui K, Shibutani M, Hase T, Kajiwara T. FEBS Lett 1996;394:21–24. [PubMed: 8925919]
24. Matsui K, Ujita C, Fujimoto S, Wilkinson J, Hiatt B, Knauf V, Kajiwara T, Feussner I. FEBS Lett 2000;481:183–188. [PubMed: 10996320]
25. Stumpe M, Kandzia R, Gobel C, Rosahl S, Feussner I. FEBS Lett 2001;507:371–376. [PubMed: 11696374]
26. Hoffman BJ, Broadwater JA, Johnson P, Harper J, Fox BG, Kenealy WR. Protein Expr Purif 1995;6:646–654. [PubMed: 8535158]
27. Imai T, Globerman H, Gertner JM, Kagawa N, Waterman MR. J Biol Chem 1993;268:19681–19689. [PubMed: 8396144]
28. Ko TP, Safo MK, Musayev FN, Di Salvo ML, Wang C, Wu SH, Abraham DJ. Acta Crystallogr D Biol Crystallogr 2000;56:241–245. [PubMed: 10666617]
29. Beers RF Jr, Sizer IW. J Biol Chem 1952;195:133–140. [PubMed: 14938361]
30. Brash AR, Baertschi SW, Ingram CD, Harris TM. J Biol Chem 1987;262:15829–15839. [PubMed: 2824470]
31. Brash AR, Porter AT, Maas RL. J Biol Chem 1985;260:4210–4216. [PubMed: 2984196]
32. Brash AR, Hughes MA, Hawkins DJ, Boeglin WE, Song WC, Meijer L. J Biol Chem 1991;266:22926–22931. [PubMed: 1744085]
33. Chang MS, Boeglin WE, Guengerich FP, Brash AR. Biochemistry 1996;35:464–471. [PubMed: 8555216]
34. Dix TA, Marnett LJ. J Biol Chem 1985;260:5351–5357. [PubMed: 3988758]
35. Gardner HW. Free Radic Biol Med 1989;7:65–86. [PubMed: 2666279]
36. Fita I, Rossmann MG. J Mol Biol 1985;185:21–37. [PubMed: 4046038]
37. Reid TJ 3rd, Murthy MR, Sicignano A, Tanaka N, Musick WD, Rossmann MG. Proc Natl Acad Sci U S A 1981;78:4767–4771. [PubMed: 6946424]
38. Vainshtein BK, Melik-Adamyan WR, Barynin VV, Vagin AA, Grebenko AI. Nature 1981;293:411–412. [PubMed: 7278994]
39. Liu J, Seibold SA, Rieke CJ, Song I, Cukier RI, Smith WL. J Biol Chem 2007;282:18233–18244. [PubMed: 17462992]
40. Song WC, Baertschi SW, Boeglin WE, Harris TM, Brash AR. J Biol Chem 1993;268:6293–6298. [PubMed: 8454602]
41. Frankel EN. Chem Phys Lipids 1987;44:73–85. [PubMed: 3311422]
42. Porter NA, Caldwell SE, Mills KA. Lipids 1995;30:277–290. [PubMed: 7609594]

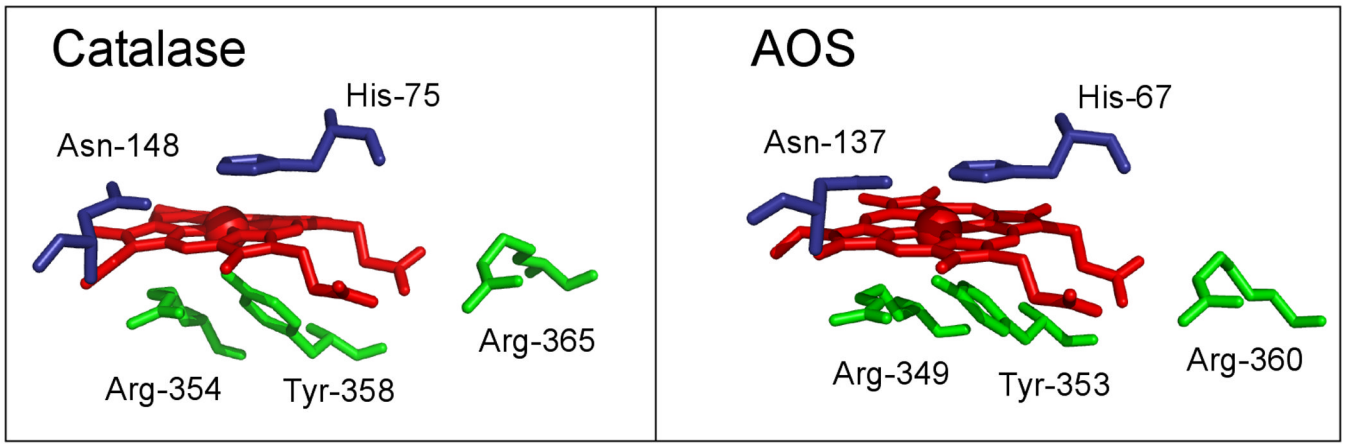

Fig. 1.

Key residues in the heme environment in the active sites of human catalase and *P. homomalla* cAOS.

The heme (red) has a conserved Asn and His residue (blue) on the distal side. The proximal heme ligand, Tyr, is flanked by two conserved Arg residues (green). The structures are from PDB files 1DGF (human catalase) and 1U5U (cAOS).

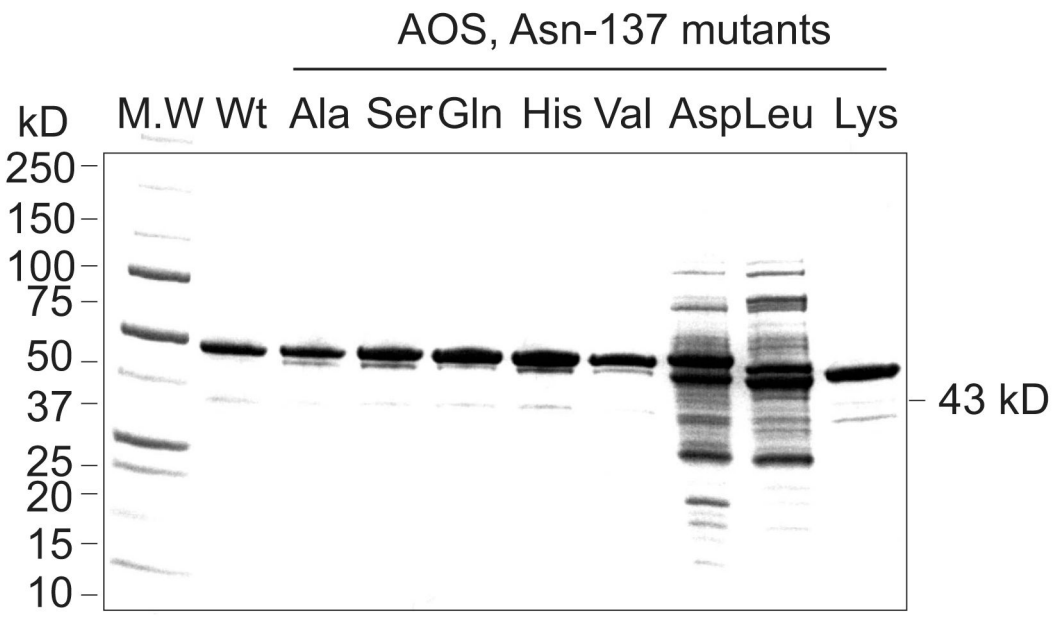

Fig. 2.

SDS -PAGE with Coomassie staining of wild type cAOS and its mutant proteins after Ni- NTA affinity chromatography. Each lane was loaded with 1–2 μg of protein, except for the Asp and Leu mutants, which were loaded with ~4 μg protein due to their lower levels of cAOS expression in *E. coli*.

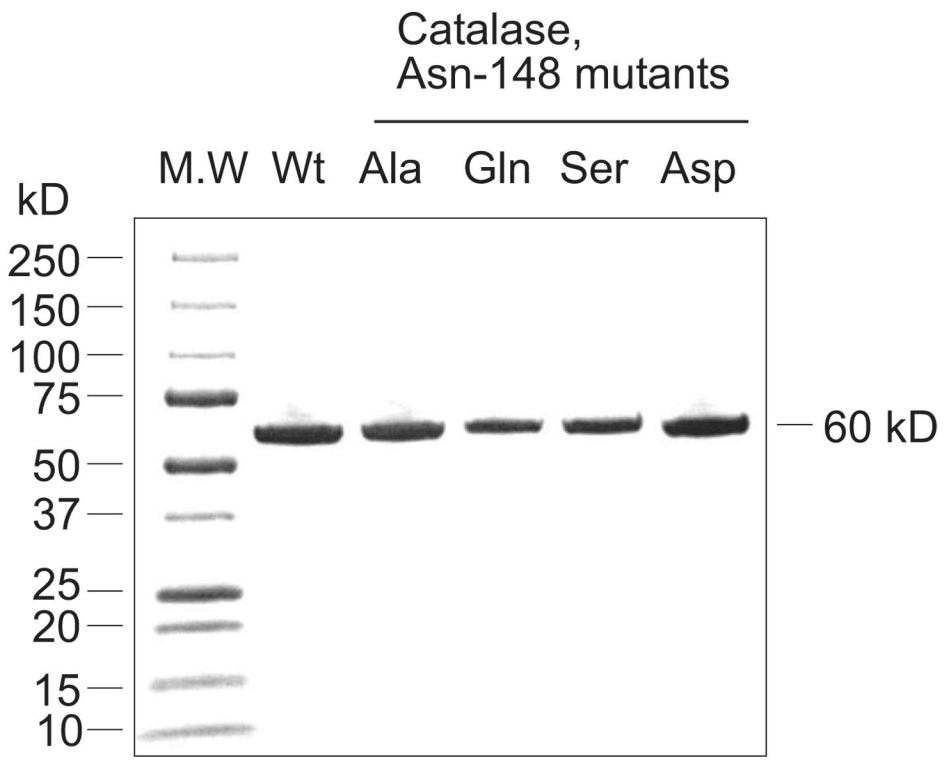

Fig. 3.
SDS-PAGE of wild type human catalase and its mutant proteins recovered from Mono-Q anion exchange chromatography.

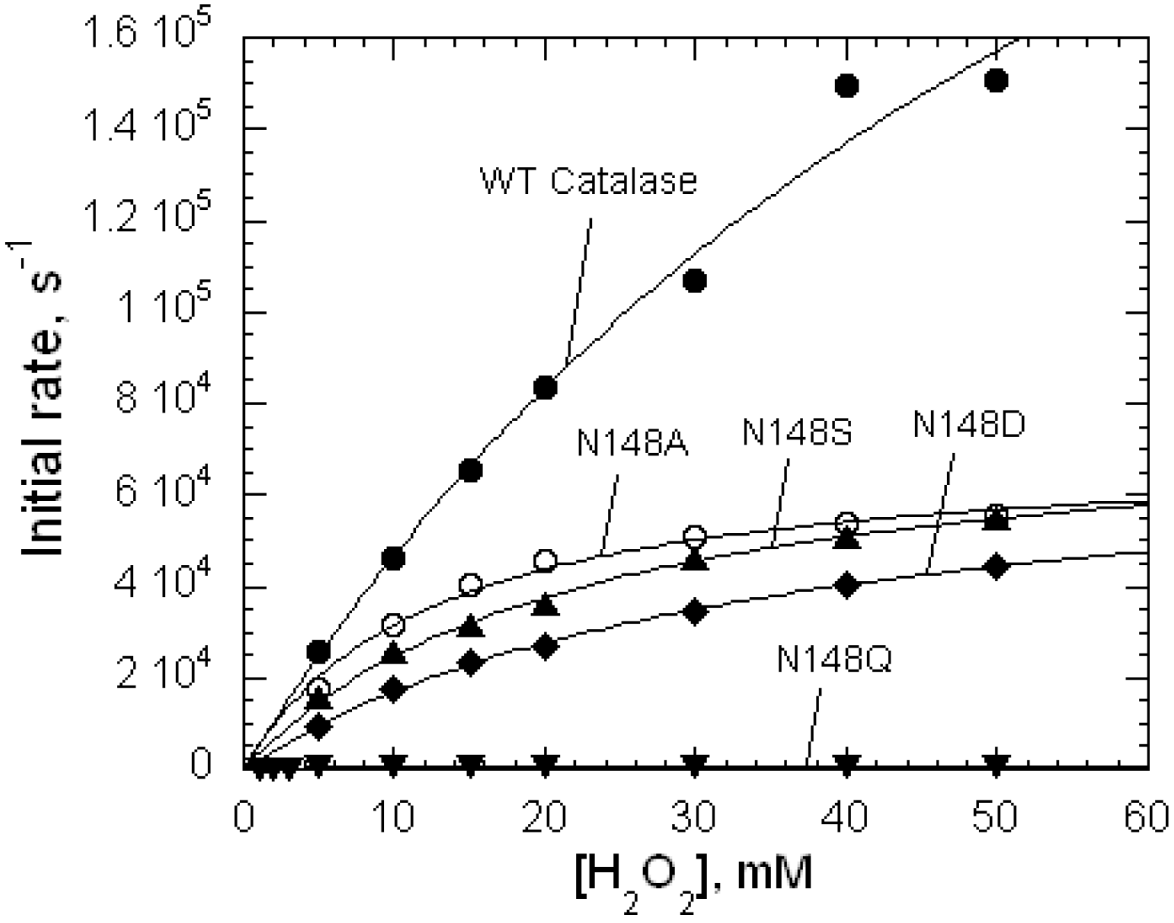

Fig. 4.

Kinetic analysis on wild type human catalase and its mutants. The initial velocity was fitted to the Michaelis-Menten equation using the KaleidaGraph (Synergy software) program.

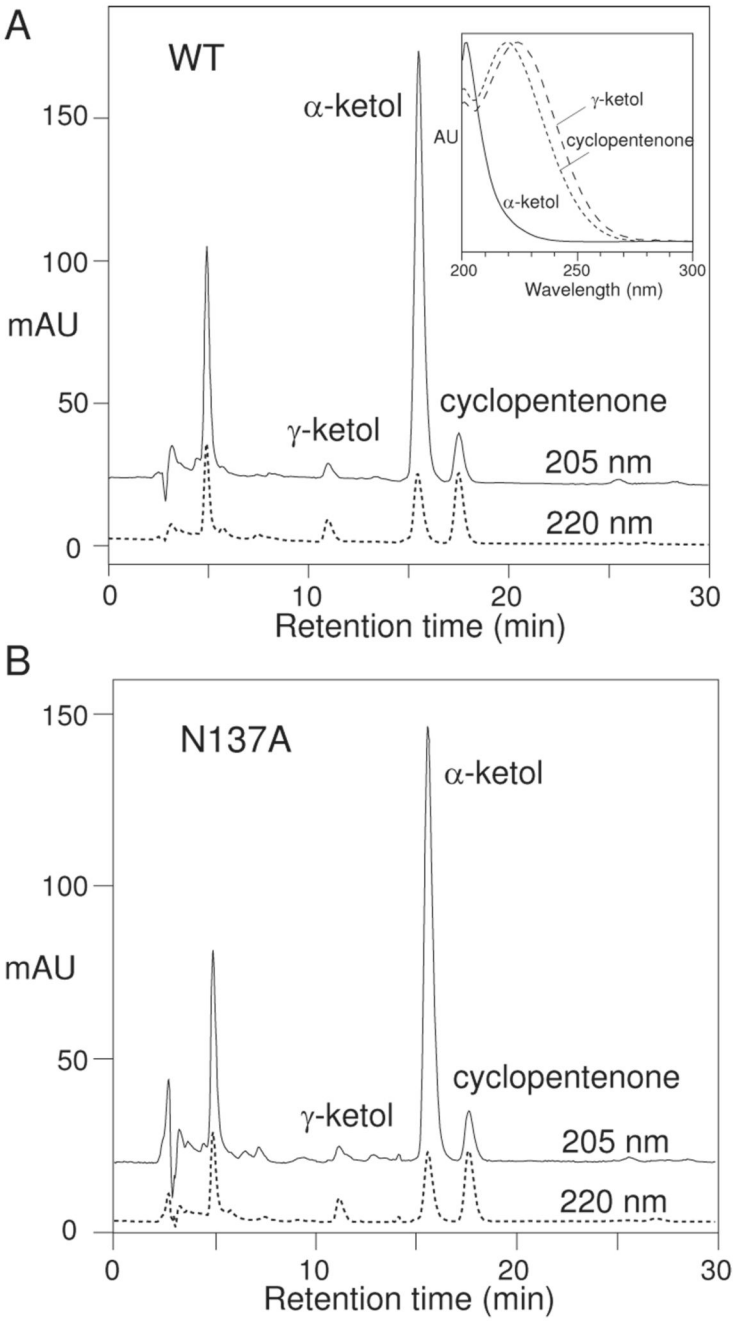

Fig. 5.

RP-HPLC analysis of products from the reaction of 8*R*-HPETE with (A) wild-type cAOS, and (B) the N137A mutant. Inset: the UV spectra of α-ketol, γ-ketol and cyclopentenone.

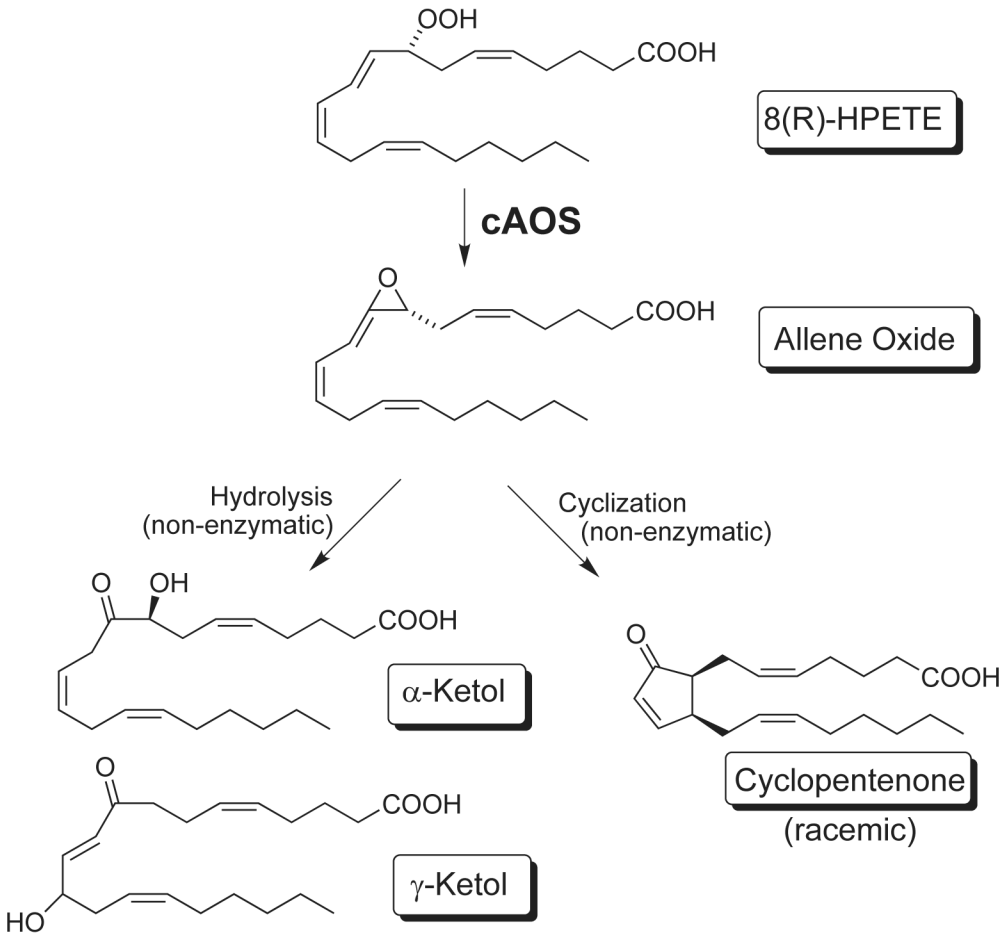

Scheme.

Table 1

Primers designed for the mutagenesis of conserved Asn in cAOS and human catalase

N148Q	5' GGT AAC TGG GAT CTC GTT GGA **CAG** AAC ACC CCC ATT TTC TTC ATC 3'
	5' GAT GAA GAA AAT GGG GGT GTT **CTG** TCC AAC GAG ATC CCA GTT ACC 3'
N148D	5' GGT AAC TGG GAT CTC GTT GGA **GAT** AAC ACC CCC ATT TTC TTC ATC 3'
	5' GAT GAA GAA AAT GGG GGT GTT **ATC** TCC AAC GAG ATC CCA GTT ACC 3'
N148A	5' GGT AAC TGG GAT CTC GTT GGA **GCT** AAC ACC CCC ATT TTC TTC ATC 3'
	5' GAT GAA GAA AAT GGG GGT GTT **AGC** TCC AAC GAG ATC CCA GTT ACC 3'
N148S	5' GGT AAC TGG GAT CTC GTT GGA **TCT** AAC ACC CCC ATT TTC TTC ATC 3'
	5' GAT GAA GAA AAT GGG GGT GTT **AGA** TCC AAC GAG ATC CCA GTT ACC 3'
N137A	5' GGT CCA CTG GAT ATC GTC ATG **GCT** ACG GGT GAA GCC AAT ATA TTT 3'
	5' AAA TAT ATT GGC TTC ACC CGT **AGC** CAT GAC GAT ATC CAG TGG ACC 3'
N137L	5' GGT CCA CTG GAT ATC GTC ATG **CTT** ACG GGT GAA GCC AAT ATA TTT 3'
	5'AAA TAT ATT GGC TTC ACC CGT **AAG** CAT GAC GAT ATC CAG TGG ACC 3'
N137H	5'GGT CCA CTG GAT ATC GTC ATG **CAT** ACG GGT GAA GCC AAT ATA TTT 3'
	5'AAA TAT ATT GGC TTC ACC CGT **ATG** CAT GAC GAT ATC CAG TGG ACC 3'
N137S	5' GGT CCA CTG GAT ATC GTC ATG **TCT** ACG GGT GAA GCC AAT ATA TTT 3'
	5' AAA TAT ATT GGC TTC ACC CGT **AGA** CAT GAC GAT ATC CAG TGG ACC 3'
N137K	5' GGT CCA CTG GAT ATC GTC ATG **AAA** ACG GGT GAA GCC AAT ATA TTT 3'
	5' AAA TAT ATT GGC TTC ACC CGT **TTT** CAT GAC GAT ATC CAG TGG ACC 3'
N137Q	5' GGT CCA CTG GAT ATC GTC ATG **CAG** ACG GGT GAA GCC AAT ATA TTT 3'
	5' AAA TAT ATT GGC TTC ACC CGT **CTG** CAT GAC GAT ATC CAG TGG ACC 3'
N137V	5' GGT CCA CTG GAT ATC GTC ATG **GTG** ACG GGT GAA GCC AAT ATA TTT 3'
	5' AAA TAT ATT GGC TTC ACC CGT **CAC** CAT GAC GAT ATC CAG TGG ACC 3'
N137D	5' GGT CCA CTG GAT ATC GTC ATG **GAT** ACG GGT GAA GCC AAT ATA TTT 3'
	5' AAA TAT ATT GGC TTC ACC CGT **ATC** CAT GAC GAT ATC CAG TGG ACC 3'

Table 2

Kinetic parameters for wild type human catalase and its mutants.

Enzyme	K_M (mM)	k_{cat} (s^{-1})	k_{cat}/K_M ($M^{-1}s^{-1}$)	R value
Catalase	71.8	3.8×10^5	5.3×10^6	0.99
N148A	12.5	7.1×10^4	5.7×10^6	0.99
N148S	21.9	7.9×10^4	3.6×10^6	0.99
N148D	33.8	7.4×10^4	2.2×10^6	0.99
N148Q	7.5	9.6×10^2	1.3×10^5	0.99

R value represents the fit to Michaelis-Menten equation.

Table 3

Activities for cAOS and its mutants with the substrate 8*R*-HPETE (40 μM)

Enzyme	Rate[a], s^{-1} (range)	% of wild type
cAOS, wild type	1603 (1309–2045)	100
N137A	69 (62–73)	4.3
N137Q	70 (50–100)	4.4
N137D	52 (41–60)	3.2
N137S	28 (22–31)	1.7
N137H	23 (21–25)	1.4
N137V	14 (13–18)	0.9
N137K	2.5 (2–3)	0.2
N137L	0.5 (0–1)	0.03

[a] mean of 3 or 4 determinations

Units of rates are nanomoles of 8*R*-HPETE per nanomole heme moiety per second.